Revista Colombiana de Cancerología

Julio - Septiembre / 2023

Rev Colomb Cancerol. 2023;27(2):389-396
https://doi.org/10.35509/01239015.957

NOTA TÉCNICA

Obtaining and characterization of spheroids using colon adenocarcinoma SW480 cells

Obtención y caracterización de esferoides utilizando células de adenocarcinoma de colon SW480

Susana Ceballos-Duque[1], María Elena Maldonado-Celis[1], Yuliet Montoya[2]

[1] Escuela de Nutrición y Dietética, Universidad de Antioquia, Medellín, Colombia.
[2] Centro de Bioingeniería, Universidad Pontificia Bolivariana, Medellín, Colombia.

Fecha de sometimiento: 20/02/2023
Fecha de aceptación: 26/06/2023
Disponible en internet: 29/09/2023

Citation:
Ceballos-Duque S, Maldonado-Celis ME, Montoya Y. Obtaining and characterization of spheroids using colon adenocarcinoma SW480 cells. Rev Col Cancerol. 2023;27(3):389-96. https://doi.org/10.35509/01239015.957

Conflicts of interest:
Los autores declaran no tener conflictos de interés.

Corresponding author:
María Elena Maldonado-Celis
Escuela de Nutrición y Dietética, Universidad de Antioquia, Medellín, Colombia.
E-mail: maria.maldonado@udea.edu.co

Resumen

El cáncer de colon ha sido estudiado convencionalmente mediante modelos *in vitro* en monocapa para entender su biología y para identificar agentes terapéuticos, pero no representan las células de un tumor que crece en tres dimensiones. Esta nota técnica presenta un protocolo para desarrollar y caracterizar un modelo tridimensional de esferoides de diferentes tamaños formados con células de adenocarcinoma de colon SW480 sembradas en micromoldes de agarosa que se dejaron crecer hasta por 21 días. Los esferoides se caracterizaron, mediante citometría de flujo, con base en el ciclo celular, función mitocondrial y apoptosis. Se encontró que esferoides de 400 µm de tamaño de siembra y tres días de crecimiento representan un modelo que posee características similares a las de los tumores *in vivo*. Se propone un método de fácil implementación para evaluar agentes terapéuticos, previo al uso de modelos animales.

Palabras clave: esferoides celulares, neoplasias del colon, muerte celular, ciclo celular, potencial de la membrana mitocondrial

Abstract

Colon cancer has conventionally been studied using in vitro monolayer models to understand its biology and identify therapeutic agents; nevertheless, they do not represent tumor cells growing in three dimensions. This technical note presents a protocol to develop and characterize a three-dimensional model of spheroids of different sizes, formed with SW480 colon adenocarcinoma cells seeded on agarose micromolds allowed to grow for up to 21 days. The spheroids were characterized by flow cytometry based on cell cycle, mitochondrial function, and apoptosis. Spheroids of 400 µm seeding size and 3 days of growth were found to represent a model possessing similar characteristics to those of tumors in vivo. An easy-to-implement method to evaluate therapeutic agents is proposed, previous to the use of animal models.

Keywords: Spheroids, cellular; colonic neoplasms; cell death; cell cycle; membrane potential, mitochondrial.

Introduction

Colon cancer is one of the leading causes of cancer death (1). Traditional two-dimensional (2D) cell culture, although advantageous (2), has limitations in mimicking real cellular environments (3), leading to the low predictive ability of pharmacological compounds (4,5). Three-dimensional (3D) cell culture methods, such as spheroids (6), have been used as an in vitro tumor model for almost 50 years and show significant similarities in drug response to animal models. Studies have found that spheroids can induce cell death, DNA damage, and quiescence in response to anticancer drugs (7,8). Additionally, the effects of natural compounds, such as quercetin, can be assessed in both 2D and 3D cultures (9). This study used the SW480 cell line due to its resemblance to features observed in other colorectal malignancies, which reflect mutational mechanisms in primary lesions (10). 3D cultures have relevance in toxicology, and numerous models have been identified (11). This study aims to develop and characterize a 3D model of colon cancer using spheroids with SW480 cells, which generate their cell matrix without needing external support (12). The model is able to maintain distinctive cellular phenotypes characteristic of tumors in vivo and is valuable for future research.

Colon adenocarcinoma spheroids

The SW480 cell line was used, as it was obtained from an adenocarcinoma, a primary tumor of a fifty-year-old Caucasian male affected by colon adenocarcinoma, which has been characterized and is considered part of an in vitro model of cancer progression since metastatic cells have been derived from it, allowing for a comparison with other studies of the differences acquired by the cells of a primary tumor when they differentiate into metastatic cells, such as those derived from SW620 (13). The subject at hand has been extensively investigated, and the findings have been documented to demonstrate that the aberrant features of this particular entity are in concordance with the predominant irregularities manifested in other colorectal malignancies. The genetic modifications observed may reflect mutational mechanisms occurring in the primary lesion cells (2).

Spheroids were prepared from a culture of SW480 cells maintained in Dulbecco's Modified Eagle Medium (DMEM) supplemented with 25 mM glucose, 2 mM L-glutamine, 10% fetal bovine serum, 100 U/ml penicillin, 100 µg/ml streptomycin, and 1% nonessential amino acids (Invitrogen, USA) to 90% confluence at 37 °C and in a humidified atmosphere with 5% CO2 (14). Cells had viability greater than 90%, as determined by trypan blue in a Neubauer chamber. Microtissues® were used, following the manufacturer's Casting, Equilibrating, and Seeding the 3D Petri Dish® protocol. The process was carried out under sterile conditions using a class II biosafety cabinet (Esco, Singapore). To prepare the microgels, 20 mg/mL ultrapure agarose (Sigma-Aldrich) was dissolved in sterile 0.9% (w/v) NaCl (saline). The solution was shaken every 10 seconds after microwave heating (1,050 W, Abba, Bogotá, Colombia) until completely clear. Then, 340 µL of dissolved agarose was deposited in the micromold and cooled for 1 minute at room temperature (RT). The gel was unmolded and transferred to a well of a 24-well plate; 500 µL of culture medium was added every 10 minutes to equilibrate the microgel. The medium was removed, and 75 µL of culture medium was deposited with different cell concentrations according to the desired spheroid seeding size (100 µm: 125 cells/75 µL; 200 µm: 1,000 cells/75 µL; 400 µm: 8,000 cells/75 µL; 600 µm: 1,500,000 cells/75 µL) (figure 1). These are estimates only. Estimates of spheroid diameter are based on the following assumptions: i) the diameter of input cells is 20 µm (4,180 µm3), ii) total spheroid volume equals cell volume times the number of input cells, iii) the spheroid is a perfect sphere, and iv) cells are perfectly distributed to all recesses. In practice, spheroid size and shape will vary depending on cell type.

Morphological characterization of SW480 spheroids

Spheroids were morphologically characterized by inverted optical microscopy (IM-3FL model, OPTIKA Microscopes, Ponteranica, BG, Italy), and images were analyzed with the OPTIKA ProView software. Images were captured with a 100x objective and at a scale of 200 µm at different time points; 20 micrographs were taken for each size (figure 2A). Images were analyzed with ImageJ 1.52v software (Wayne Rasband, National Institutes of Health, USA). Statistics were calculated using GraphPad

Prism 9.0.0. One-way ordinary ANOVA and Tukey's multiple comparisons tests were performed. Spheroids showed an increase in opaque areas from day 3 of growth. Disintegration was observed at the edges of the spheroids from day 14 and maintained until day 21. The 100 µm spheroids showed a statistically significant decrease of one area on days 3, 7, and 14 compared to day 1; on day 21, the spheroids returned to their initial area value (figure 2B). The 200 µm spheroids did not show a statistically significant decrease (figure 2C). The 400 and 600 µm spheroids showed statistically significant growth on days 3 and 7, compared to day 1, and a decrease in the area that remained constant (plateau) on days 14 and 21 (figures 2D-E).

Cell cycle analysis

To determine the distribution of the cells composing the spheroids, DNA staining with propidium iodide (PI) was performed (15); 400 and 600 µm spheroids were seeded. After 1, 3, and 7 days of growth, spheroids were recovered and mechanically disintegrated. Cell suspensions were washed with PBS at RT. Subsequently, the cells were fixed for 1 hour with cold 70% ethanol and washed again with PBS. The fixed cells were suspended in 200 µL of PBS and 250 µg/ml RNAsa; 10 µg/mL PI was added. Cells were incubated at RT for 30 minutes in the dark. Data for at least 10,000 events per sample were collected by flow cytometry and analyzed using the FlowJo™ software (v.7.6.2, Becton, Dickinson and Company, Ashland, Oregon, USA) at 488 nm excitation; emission was detected at 610/15 nm. Statistics were calculated using GraphPad Prism 9.0.0. A two-way ANOVA and a Bonferroni multiple comparisons test were performed. Figures 3A and 3B show a significant increase in the percentage of dead or dying cells in the 400 µm spheroids on days 3 and 7 compared to day 1, with a corresponding increase in the percentage of senescent-phase cells on day 3 and a decrease on day 7.

The percentage of cells in the proliferative S-phase decreased significantly on days 3 and 7 compared to day 1. In addition, cells in the proliferative G2 phase showed a decreasing trend on day 3, with a statistically significant reduction on day 7 compared to day 1. Figure 4 shows the distribution of cells in each phase of the 600 µm spheroid cell cycle over the days of growth. Figures 4A and 4B indicate a statistically significant increase in the percentage of dead or dying cells (SubG1) on days 3 and 7 compared to day 1, while the percentage of senescent (G1), proliferative (S), and proliferative cells in G2 significantly decreased on days 3 and 7 compared to day 1 of growth. Based on these findings, subsequent experiments were performed using spheroids of 400 µm in size, which were grown for 3 days.

Mitochondrial function in spheroid cells

Fluorescent probes, such as DiOC6 and PI, can be used to assess changes in membrane potential and plasma membrane damage. Hyperpolarized mitochondria accumulate more cation dye, whereas depolarized mitochondria accumulate less (16). The 400 µm spheroids were seeded as described in figure 1. After 1 and 3 days of growth, they were mechanically disintegrated using a vortex shaker (Velp Scientifica, Usmate Velate MB, Italy) at 8,000 rpm for 5 minutes; then, the sample was homogenized gently using a pipette. They were incubated with DiOC6 at 50 nM and 10 nM of PI at 1 mg/mL for 30 minutes in the dark at RT. Data for at least 10,000 events per sample were collected by flow cytometry and analyzed using the FlowJo™ software (v7.6.2) at 488 nm excitation; emission was detected with a green filter at 530/15 nm for DiOC6 and 610/15 nm for PI. Statistics were calculated using GraphPad Prism 9.0.0. A two-way ANOVA and Tukey's multiple comparisons test were performed. Figures 5A and 5B show a significant decrease in the percentage of viable cells in the 400 µm spheroids after 3 days of growth compared to those after one day. In addition, a statistically significant increase in the percentage of apoptotic cells without mitochondrial dysfunction is observed over time.

Apoptotic cells in spheroids

During apoptosis, phosphatidylserine (PS) translocates to the outer membrane, which can be detected by annexin V, a protein with high affinity and selectivity for PS. Double staining of cells with annexin V-fluorescein isothiocyanate (FITC) and PI can differentiate between necrotic, late apoptotic, early apoptotic, and viable cells (17). The 400 µm spheroids were obtained as described in figure 1. After 1 and 3 days of growth, they were mechanically disintegrated as explained above and mixed with 1 mL of annexin V-binding buffer (10

mM HEPES; 0.14 M NaCl; 2.5 mM CaCl2; pH 7.4), 4 µl of annexin V/FITC, and 10 µL of PI at 1 mg/mL. Samples were incubated for 15 minutes at 4 °C in the dark. Data from at least 10,000 events per sample were analyzed by flow cytometer (LSR Fortessa™, BD Biosciences, USA), using the FlowJo™ software (v7.6.2) at 488 nm excitation; emission was detected at 610/15 nm for PI and 518 nm for annexin V/FITC and analyzed. Figure 6A shows the cell distribution in each quadrant after 1 and 3 days of spheroid growth. Figure 6B demonstrates that 400 µm spheroids grown for 3 days, compared to those grown for 1 day, had a significant increase in apoptotic cells, including early and late phases, and a significant decrease in viable cells, as observed in prior experiments.

Conclusions

A spheroid model was obtained from SW480 colon adenocarcinoma cells of different seeding sizes and days of growth. Morphological analysis, cell cycle, mitochondrial function, and apoptosis showed that spheroids with a seeding size of 400 µm and 3 days of growth exhibit exponential growth with a decrease in viable cells, increase in apoptotic cells, and no mitochondrial damage. This suggests that this model resembles tumors in vivo. Furthermore, it should be noted that the process of obtaining spheroids from SW480 cells is a strategy for evaluating therapeutic agents before using preclinical animal models.

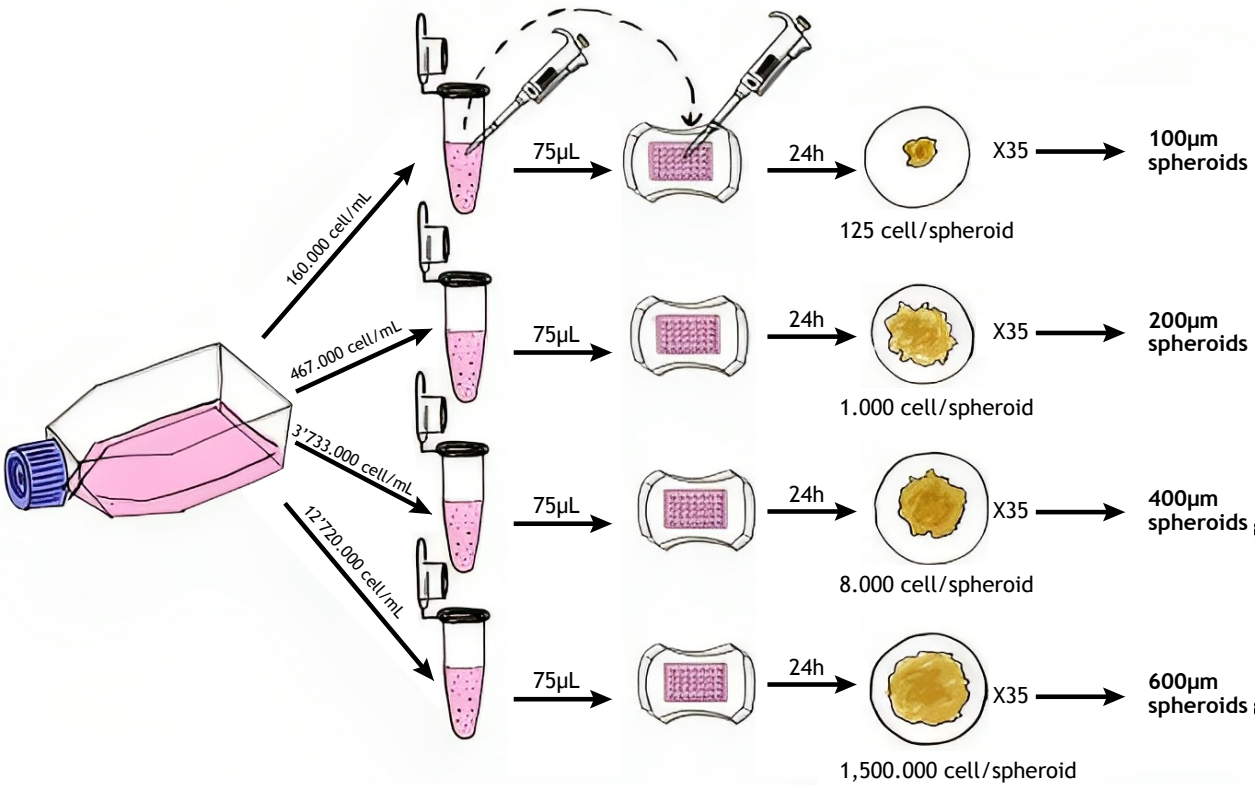

Figure 1. Cell seeding process for spheroid formation.

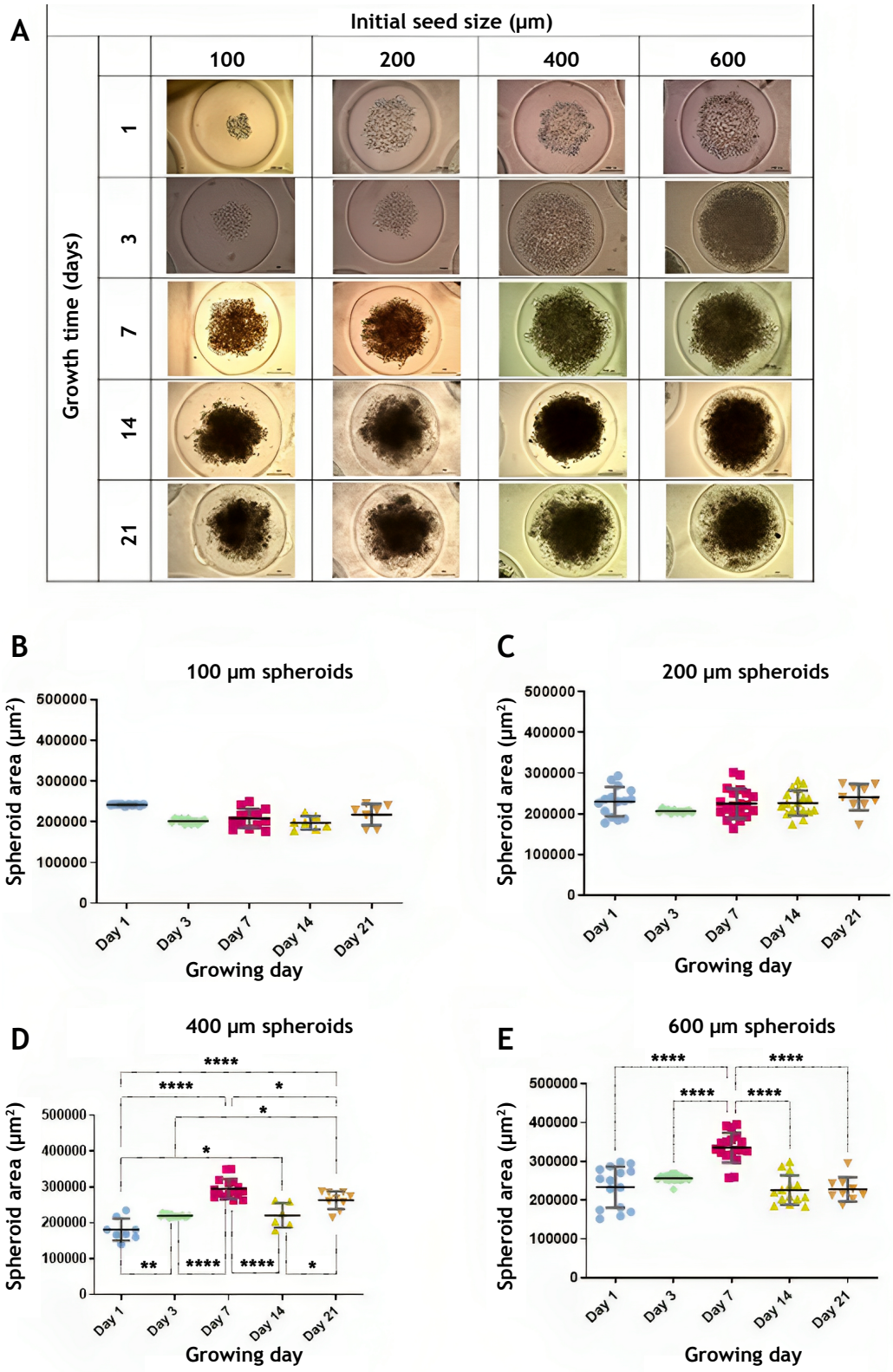

Figure 2. Morphological characterization of different spheroids (100, 200, 400, and 600 µm) at different growth times (1, 3, 7, 14, and 21 days). **A.** Micrographic registration. **B-E.** Area of 100, 200, 400, and 600 µm spheroids. *p≤0.01; **p≤0.001; ***p≤0.0001; ****p≤0.00001.

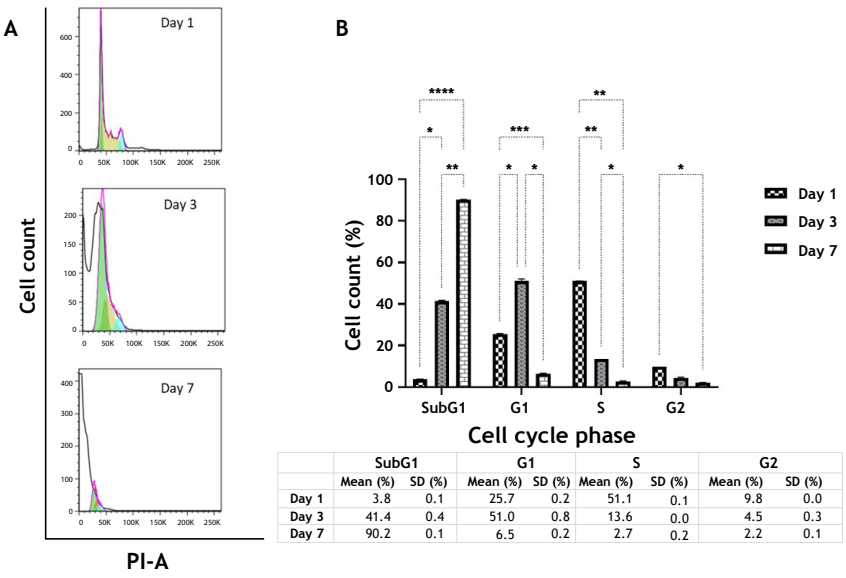

	SubG1		G1		S		G2	
	Mean (%)	SD (%)	Mean (%)	SD (%)	Mean (%)	SD (%)	Mean (%)	SD (%)
Day 1	3.8	0.1	25.7	0.2	51.1	0.1	9.8	0.0
Day 3	41.4	0.4	51.0	0.8	13.6	0.0	4.5	0.3
Day 7	90.2	0.1	6.5	0.2	2.7	0.2	2.2	0.1

PI-A=Propidium iodide-annexin; SD=Standard deviation; SubG1=Sub-Gap 1 phase; G1=Gap 1 phase; S=Synthesis phase; G2=Gap 2 phase.

Figure 3. Cell cycle analysis of 400 µm SW480 spheroids at three different times of growth (1, 3, and 7 days). Approximately 35 spheroids and ≈10,000 events were evaluated for each condition. **A.** Representative histograms of the distribution of events in each cell cycle phase. **B.** Bar chart with the standard deviation of the mean of three independent experiments. *p≤0.01; **p≤0.001; ***p≤0.0001; ****p≤0.00001.

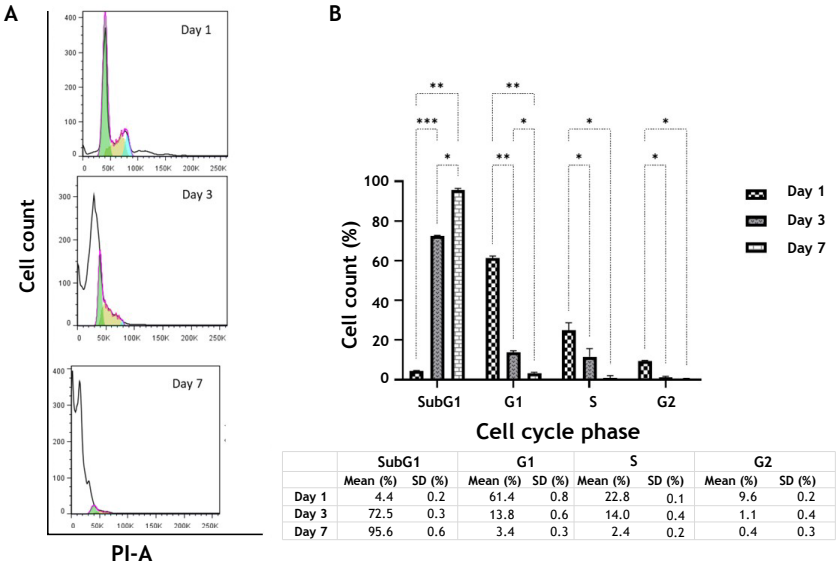

	SubG1		G1		S		G2	
	Mean (%)	SD (%)	Mean (%)	SD (%)	Mean (%)	SD (%)	Mean (%)	SD (%)
Day 1	4.4	0.2	61.4	0.8	22.8	0.1	9.6	0.2
Day 3	72.5	0.3	13.8	0.6	14.0	0.4	1.1	0.4
Day 7	95.6	0.6	3.4	0.3	2.4	0.2	0.4	0.3

PI-A=Propidium iodide-annexin; SD=Standard deviation; SubG1=SubG1=Sub-Gap 1 phase; G1=Gap 1 phase; S=Synthesis phase; G2=Gap 2 phase.

Figure 4. Cell cycle analysis of 600 µm SW480 spheroids at three different time of growth (1, 3, and 7 days). Approximately 35 spheroids and 10,000 events were evaluated for each condition. **A.** Representative histograms of the distribution in each cell cycle phase. **B.** Bar chart with the standard deviation of the mean of three independent experiments. *p≤0.01; **p≤0.001; ***p≤0.0001.

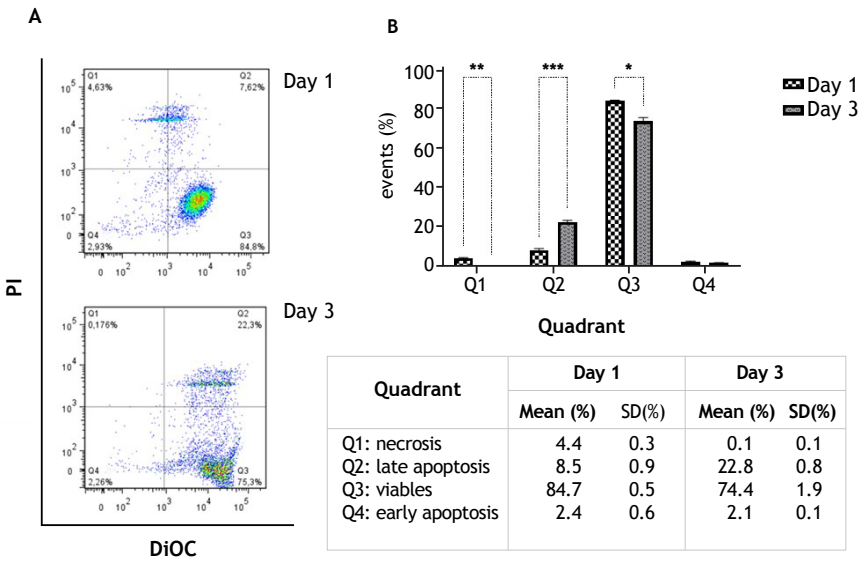

Quadrant	Day 1		Day 3	
	Mean (%)	SD(%)	Mean (%)	SD(%)
Q1: necrosis	4.4	0.3	0.1	0.1
Q2: late apoptosis	8.5	0.9	22.8	0.8
Q3: viables	84.7	0.5	74.4	1.9
Q4: early apoptosis	2.4	0.6	2.1	0.1

PI=Propidium iodide; DiOC6= 3,3'-dihexyloxacarbocyanine iodide; SD=Standard deviation; Q1=Quadrant 1; Q2=Quadrant 2; Q3=Quadrant 3; Q4=Quadrant 4.

Figure 5. Determination of the mitochondrial membrane potential of 400 µm SW480 spheroids on days 1 and 3 of growth. Approximately 35 spheroids were evaluated for each condition. **A.** Representative dot plot of spheroids (10,000 events). **B.** Bar chart with the standard deviation of the mean of three independent experiments. The table shows the percentage of cells in the quadrants: Q1 (DiOC6−/PI+); Q2 (DiOC6+/PI+); Q3 (DiOC6+/PI−); Q4 (DiOC6−/PI−). *p≤0.01; **p≤0.001; ***p≤0.0001.

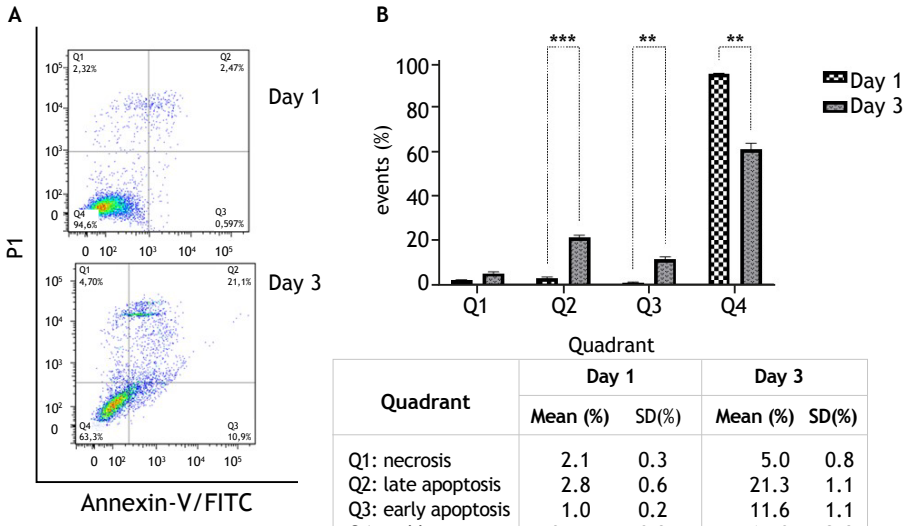

Quadrant	Day 1		Day 3	
	Mean (%)	SD(%)	Mean (%)	SD(%)
Q1: necrosis	2.1	0.3	5.0	0.8
Q2: late apoptosis	2.8	0.6	21.3	1.1
Q3: early apoptosis	1.0	0.2	11.6	1.1
Q4: viables	94.4	0.3	61.0	2.8

PI=Propidium iodide; FITC=Fluorescein isothiocyanate; SD=Standard deviation; Q1=Quadrant 1; Q2=Quadrant 2; Q3=Quadrant 3; Q4=Quadrant 4.

Figure 6. Apoptotic cell analysis of 400 µm SW480 spheroids on days 1 and 3 of growth. Approximately, 35 spheroids were evaluated for each condition. **A.** Representative dot plot of spheroids (10,000 events). **B.** Bar chart with the standard deviation of the mean of three independent experiments. The table shows the percentage of cells in the quadrants: Q1 (Annexin−/PI+); Q2 (Annexin+/PI+); Q3 (Annexin+/PI−); Q4 (Annexin−/PI−). *p≤0.01; **p≤0.001.

References

1. Sung H, Ferlay J, Siegel RL, Laversanne M, Soerjomataram I, Jemal A, *et al*. Global Cancer Statistics 2020: GLOBOCAN estimates of incidence and mortality worldwide for 36 cancers in 185 countries. CA Cancer J Clin. 2021;71(3):209-49. https://doi.org/10.3322/caac.21660

2. Mazzoleni G, Di Lorenzo D, Steimberg N. Modelling tissues in 3D: the next future of pharmaco-toxicology and food research? Genes Nutr. 2009;4(1):13-22. https://doi.org/10.1007/s12263-008-0107-0

3. Imamura Y, Mukohara T, Shimono Y, Funakoshi Y, Chayahara N, Toyoda M, *et al*. Comparison of 2D- and 3D-culture models as drug-testing platforms in breast cancer. Oncol Rep. 2015;33(4):1837-43. https://doi.org/10.3892/or.2015.3767

4. Lovitt CJ, Shelper TB, Avery VM. Advanced cell culture techniques for cancer drug discovery. Biology. 2014;3(2):345-67. https://doi.org/10.3390/biology3020345

5. Breslin S, O'Driscoll L. Three-dimensional cell culture: the missing link in drug discovery. Drug Discov Today. 2013;18(5-6):240-9. https://doi.org/10.1016/j.drudis.2012.10.003

6. Kapałczyńska M, Kolenda T, Przybyla W, Zajaczkowska M, Teresiak A, Filas V, *et al*. 2D and 3D cell cultures – a comparison of different types of cancer cell cultures. Arch Med Sci. 2018;14(4):910-9. https://doi.org/10.5114/aoms.2016.63743

7. Ravi M, Paramesh V, Kaviya SR, Anuradha E, Paul Solomon FD. 3D cell culture systems: advantages and applications. J Cell Physiol. 2015;230(1):16-26. https://doi.org/10.1002/jcp.24683

8. Virgone-Carlotta A, Lemasson M, Mertani HC, Diaz J-J, Monnier S, Dehoux T, *et al*. In-depth phenotypic characterization of multicellular tumor spheroids: Effects of 5-fluorouracil. PLoS One. 2017;12(11):e0188100. https://doi.org/10.1371/journal.pone.0188100

9. Moreno-Londoño AP, Castañeda-Patlán MC, Sarabia-Sánchez MA, Macías-Silva M, Robles-Flores M. Canonical Wnt pathway is involved in chemoresistance and cell cycle arrest induction in colon cancer cell line spheroids. Int J Mol Sci. 2023;24(6):5252. https://doi.org/10.3390/ijms24065252

10. Tomita N, Jiang W, Hibshoosh H, Warburton D, Kahn SM, Weinstein IB. Isolation and characterization of a highly malignant variant of the SW480 human colon cancer cell line. Cancer Res. 1992;52(24):6840-7. PMID: 1458472

11. Pognan F, Beilmann M, Boonen HCM, Czich A, Dear G, Hewitt P, *et al*. The evolving role of investigative toxicology in the pharmaceutical industry. Nat Rev Drug Discov. 2023;22(4):317-35. https://doi.org/10.1038/s41573-022-00633-x

12. Baião A, Dias S, Soares AF, Pereira CL, Oliveira C, Sarmento B. Advances in the use of 3D colorectal cancer models for novel drug discovery. Expert Opin Drug Discov. 2022;17(6):569-80. https://doi.org/10.1080/17460441.2022.2056162

13. Hewitt RE, McMarlin A, Kleiner D, Wersto R, Martin P, Tsokos M, *et al*. Validation of a model of colon cancer progression. J Pathol. 2000;192(4):446-54. https://doi.org/10.1002/1096-9896(2000)9999:9999%3C::aid-path775%3E3.0.co;2-k

14. Maldonado ME, Bousserouel S, Gossé F, Minker C, Lobstein A, Raul F. Differential induction of apoptosis by apple procyanidins in TRAIL-sensitive human colon tumor cells and derived TRAIL-resistant metastatic cells. J Cancer Mol. 2009;5(1):21-30. Available from: https://bibliotecadigital.udea.edu.co/bitstream/10495/21982/3/MaldonadoMaria_2009_DifferentialInductionApoptosis.pdf

15. Ramirez V, Arango SS, Maldonado ME, Uribe D, Aguillón JA, Quintero JP, *et al*. Biological activity of *Passiflora edulis f. flavicarpa* ethanolic leaves extract on human colonic adenocarcinoma cells. J Appl Pharm Sci. 2019;9(02):64-71. Available from: http://hdl.handle.net/20.500.12622/3232

16. Cottet-Rousselle C, Ronot X, Leverve X, Mayol JF. Cytometric assessment of mitochondria using fluorescent probes. Cytometry A. 2011;79(6):405-25. https://doi.org/10.1002/cyto.a.21061

17. Crowley LC, Marfell BJ, Scott AP, Waterhouse NJ. Quantitation of apoptosis and necrosis by annexin V binding, propidium iodide uptake, and flow cytometry. Cold Spring Harb Protoc. 2016;2016(11):953-7. https://doi.org/10.1101/pdb.prot087288